Investigation into the Material Composition of the Meteorite 94:0097

Mariam Andersson

July 6, 2011

1 Introduction

Material analysis of meteorites can give clues as to what the solar system was initially composed of [1]. The abundance of elements in meteorites should correspond to the isotopic abundance in the dust and gas that the solar system is believed to have formed from. Evidence for this can be found in the fact that the isotopic abundance for elements heavier than oxygen in the photosphere of the sun matches the abundance of elements in meteorites [2].When differentiated asteroids collide with other objects, fragments from their cores can be ejected; these fragments are known as "iron meteorites" when they reach the Earth [3]. The composition of iron meteorites is believed to give insight into the composition of the Earth's core [4].

This investigation deals with the elemental composition of an iron meteorite: which elements a meteorite is composed of and also, the quantity of these elements.

2 Background Information

The coarse octahedrite iron meteorite used in the investigation was found in 1840 in Smithville, De Kalb County, Tennessee, U.S.A. Its catalogue number is 94:0097.

Neutron activation analysis is a method used to verify the concentrations of elements in a substance. A sample is exposed to a neutron flow causing the nuclei in the sample to absorb neutrons by neutron capture, producing unstable radioactive isotopes of the original nuclides. The neutrons also transfer energy to the nucleus, causing it to emit instant gamma radiation (photons). The radioactive isotopes then decay by emitting alpha or beta radiation. Following such decays, excited states in the daughter nucleus can be populated. When these nuclei de-excite to the ground state, 'delayed' gamma radiation is emitted. The gamma rays emitted by the nuclei are specific to certain isotopes, meaning that each radioactive isotope will emit gamma radiation at one or several definite energy levels unique to that isotope. It is this property that allows for the identification of isotopes by analysis of the gamma rays emitted.

The radiation naturally present in the Earth's environment is known as background radiation. This can be emitted from both natural and artificial sources e.g. building walls or space. Care must be taken not to mistake gamma radiation owing to the background radiation as gamma radiation emitted by a sample when dealing with gamma-ray spectroscopy.

In order to analyse the gamma rays, they must first be detected. In this case, a germanium detector was used to detect the gamma radiation. A germanium detector is a "small, but very precise, electromagnetic calorimeter" capable of measuring the energy of photons (gamma rays) [5]. The Germanium detector, however, is limited as to how accurately it can measure the number of photons emitted at various energy levels. For example, there may be 100 photons emitted at an energy of $1{,}600keV$ over a certain period of time from a source, but it is possible that the detector only detects 10 of these; this means that the detector has a 0.1 or 10% efficiency at $1{,}600keV$. An efficiency curve can be constructed for a certain detector, showing the detector's efficiency over a range of energies. Below is shown the efficiency curve obtained for the germanium detector used in this investigation.

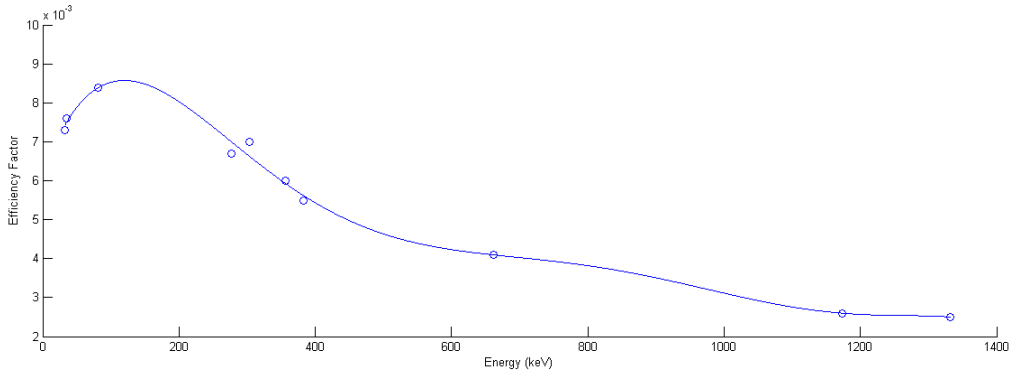

Figure 1: A Graph to show how the Efficiency of the Germanium Detector used in the Investigation Varied over a Range of Photon Energies. *The y-axis depicts the 'factor' of efficiency e.g. a factor of* 0.007 *represents* 0.7%.

A reference is made in the appendix to how the graph was obtained through measurement. Ideally, there should not be a rise in the trend line between the energies of $650keV$ and $1050keV$. The efficiency graph is used in the calculations concerning the quantity of each element in the meteorite.

Lastly, this investigation makes the assumption that the percentage abundance of isotopes in space is the same as that on Earth to allow for calculation of the relative quantities of different elements.

3 Hypothesis

The meteorite used in the investigation is classed as a coarse octahedrite iron meteorite. Coarse octahedrites contain between 6.5% to 8.8% nickel [6]. The remaining material is typically comprised of iron and and "a few tenths of percent" of Cobalt, along with trace amounts of rare metals such as platinum, gold and iridium [7]. For these reasons, it was hypothesized that the meteorite would contain approximately 7% nickel and 93% iron, with trace amounts of platinum, cobalt, gold and iridium. Considering that the mass of the meteorite is $88.4g$ this would entail that there would be in the order of $6g$ of nickel and $82g$ of iron, with smaller masses of cobalt, platinum, gold and iridium.

4 Method and Materials

A germanium detector was placed inside a lead shielding and connected to a nearby computer which used the program Maestro-32 to continuously plot spectra. Before conducting measurements on the meteorite, the background radiation that could penetrate the lead shield protecting the germanium detector had to be determined. A comprehensive background spectrum was obtained through simply taking a 'null measurement' without a sample at the detector - to acquire a spectrum with statistically significant peaks, the background measurement was performed for approximately 22 hours.

The meteorite was activated by hanging it in the vicinity of a neutron source submerged in water in a cage crafted from stainless steel wire specifically for the purpose of this investigation. The fact that the neutron source was emerged in water 'moderated' the neutrons to ensure that the majority were so called 'thermal neutrons' to increase the probability of the neutrons being absorbed by the nuclei. The meteorite was activated continuously for a little over 44 hours.

Upon removal of the meteorite from the neutron source, it was immediately placed by the germanium detector and measurements were commenced. Several separate measurements were taken to allow for

the detection of the presence of isotopes with varying half lives. A shorter measurement, for example, allows more easily for the detection of statisticallly significant peaks from isotopes with very short half lives, whereas a longer measurement is more suited to detecting the presence of longer-lived isotopes. Measurements were taken for the first 5.0 minutes, then subsequently the proceeding 34 minutes and after this, 44 hours. These measurements gave spectra with the energy of the detected photons on the x-axis and the number (counts) of photons detected on the y-axis.

For photos of the experimental set-up, refer to the appendix.

5 Results

Each spectrum obtained from the measurements initially had 'counts' on the y-axis and energy on the x-axis. Seeing as the measurements had been taken over varying durations of time, the spectra were time-standardized in the program Matlab for comparison purposes such that 'counts' was replaced with 'activity' in Bequerels (counts per second) on the y-axis. The background spectrum was then layered or laid on top of each spectrum derived from the meteorite in Matlab such that any peaks unique to the meteorite would appear above the background spectrum and could that way easily be singularized.

The peaks unique to the meteorite could then be searched for and identified as coming from certain isotopes using Lunds Nuclear Database [8]. One criterion for the search was that the gamma ray had to have been emitted from an isotope that could be created from the thermal neutron capture of a single neutron by a stable isotope; that is to say - the radioactive isotope emitting the gamma ray(s) would have had to have been directly to the right of a stable isotope in the nuclide chart [9].

The peaks that are the most likely to be significant and not simply fluctuations in the measurements exhibit Gaussian distribution (as opposed to simply being one straight line) as a result of the resolution of the germanium detector. The most significant peaks that were identified and that were used for calculations are shown below.

5.1 Graphs

5.1.1 ^{59}Fe peak at $1100keV$

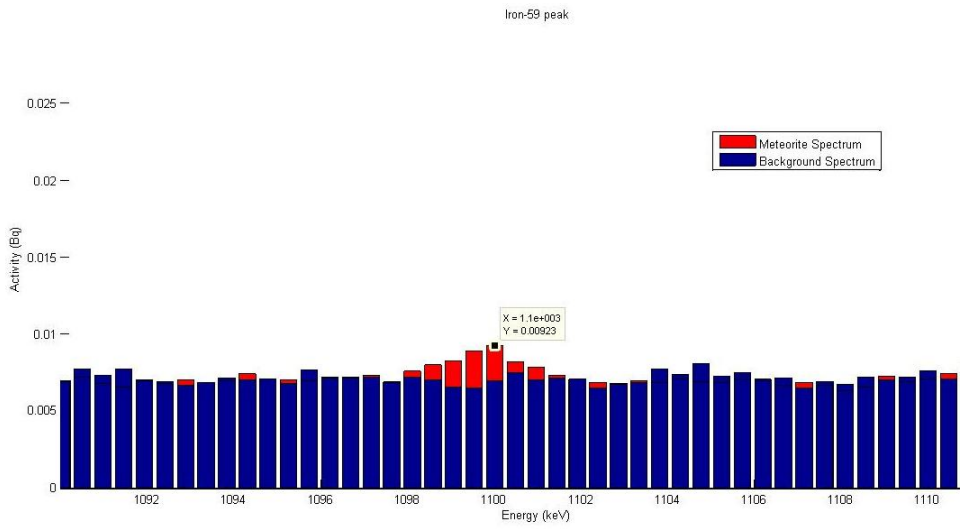

Figure 2: A graph to show the $1100keV$ peak caused by the decay of ^{59}Fe. This peak appeared in the long 44 hour measurement.

5.1.2 ^{59}Fe peak at $1292keV$

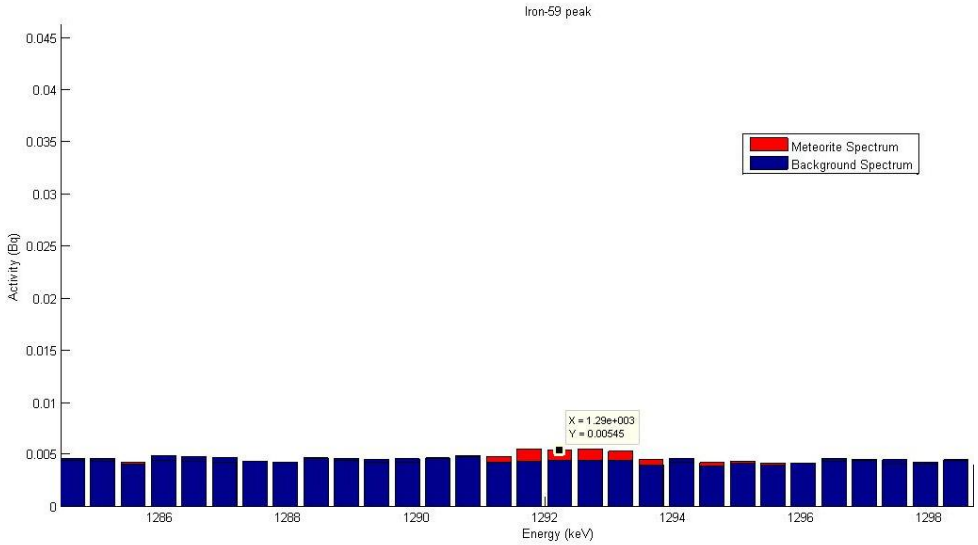

Figure 3: A graph to show the $1292keV$ peak caused by the decay of^{59}Fe . This peak appeared in the long 44 hour measurement.

5.1.3 ^{60}Co peak at $1173keV$

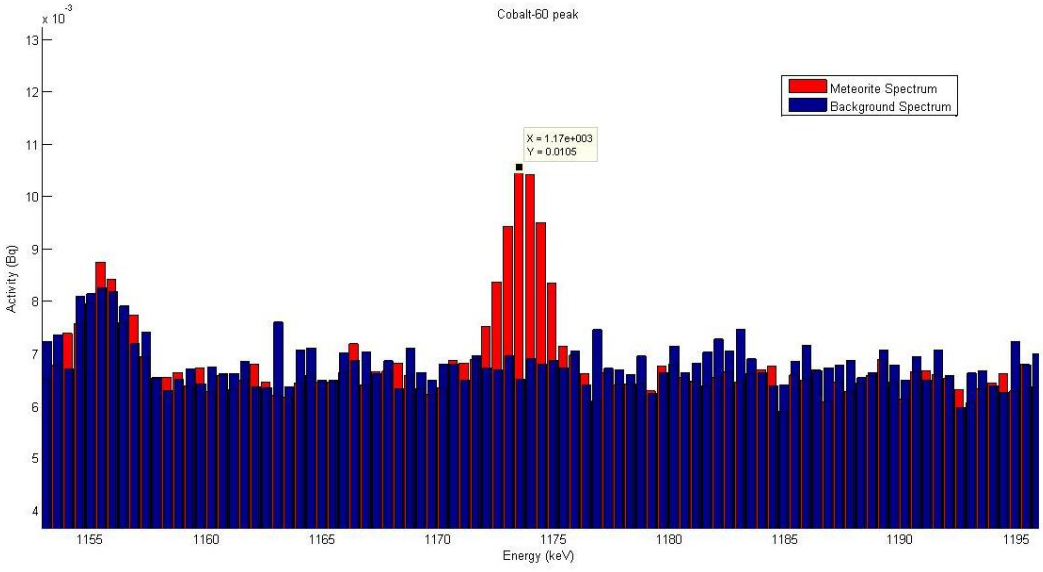

Figure 4: A graph to show the $1173keV$ peak caused by the decay of^{60}Co. This peak appeared in the long 44 hour measurement.

5.1.4 ^{60}Co peak at $1333keV$

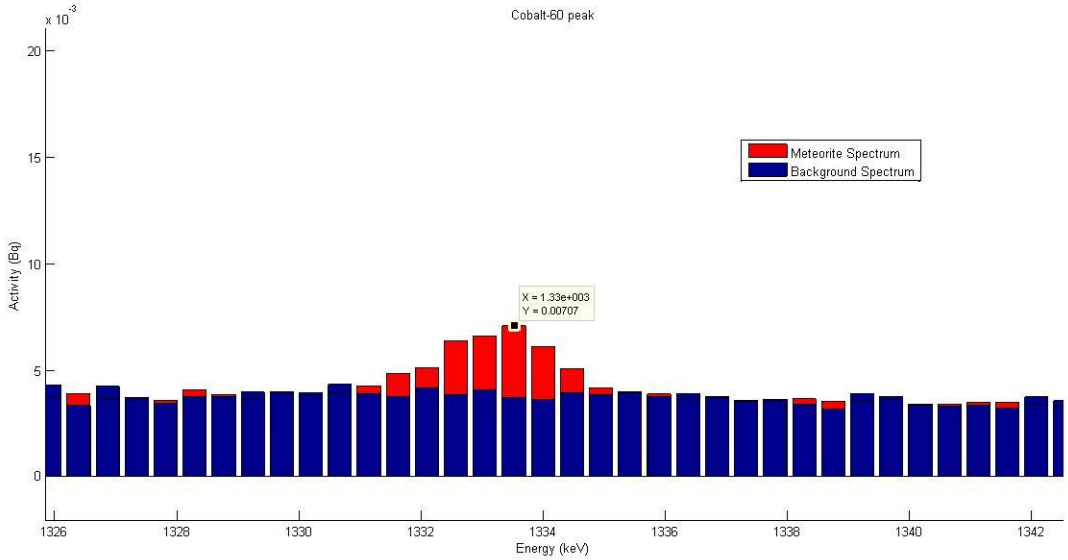

Figure 5: A graph to show the $1333keV$ peak caused by the decay of^{60}Co. This peak appeared in the long 44 hour measurement.

5.1.5 ^{56}Mn peak at $847keV$

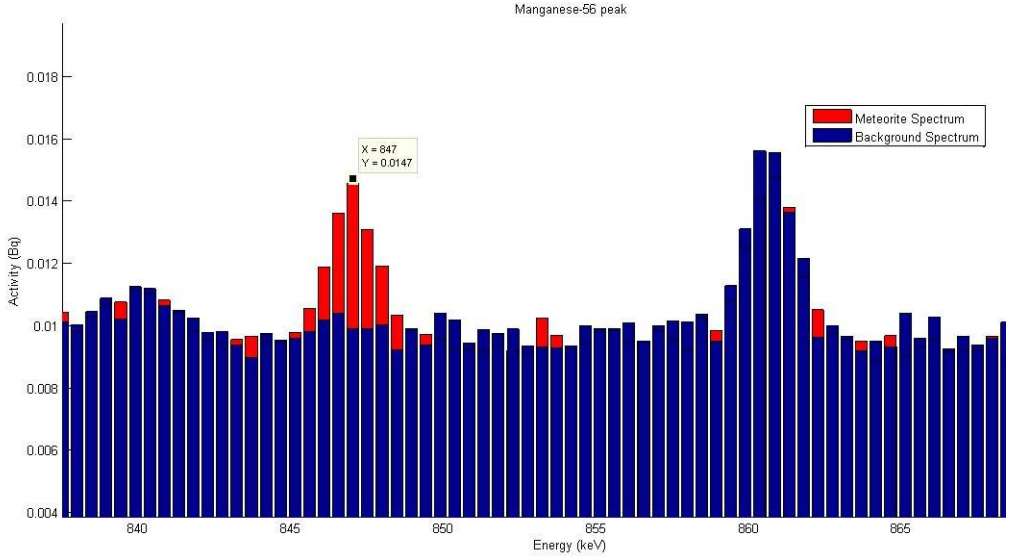

Figure 6: A graph to show the $847keV$ peak caused by the decay of^{56}MnThis peak appeared in the long 44 hour measurement.

5.1.6 ^{56}Mn peak at $1812keV$

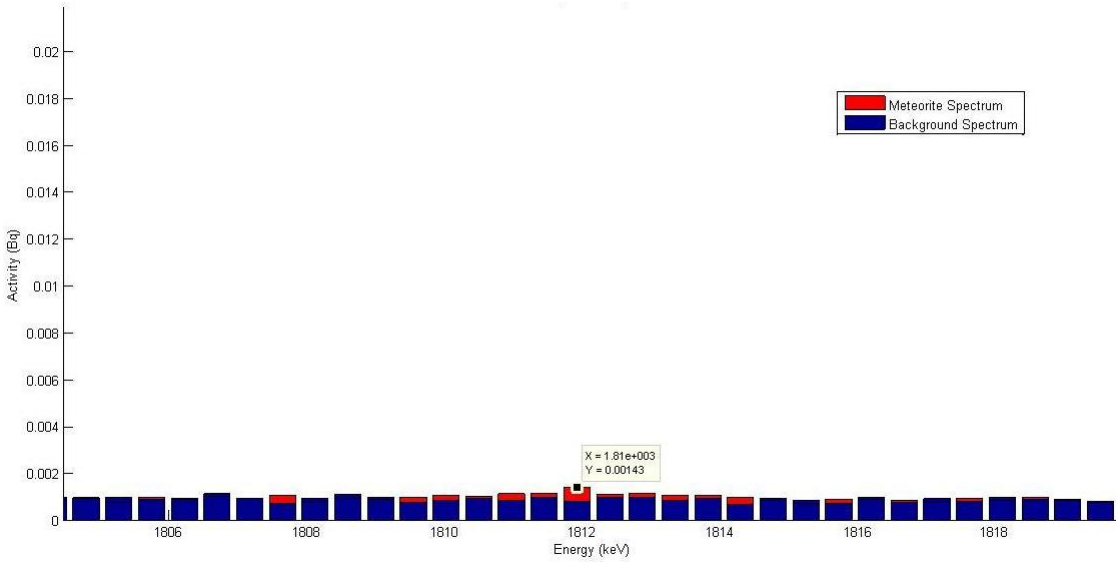

Figure 7: A graph to show the peak$1812keV$ caused by the decay of^{56}Mn. This peak appeared in the long 44 hour measurement.

5.1.7 ^{65}Ni peak at $1116keV$

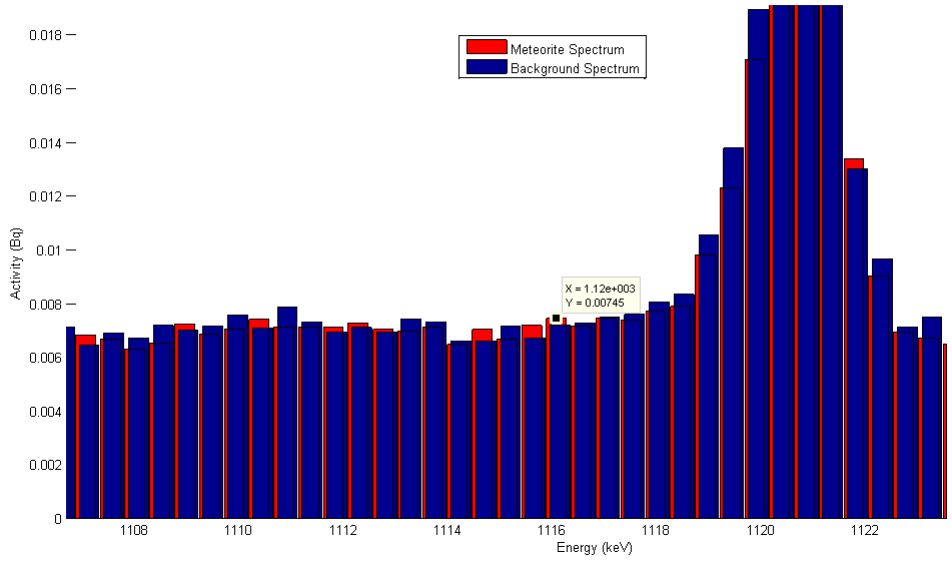

Figure 8: A graph to show the $1116keV$ peak caused by the decay of^{65}Ni. This peak appeared in the long 44 hour measurement.

5.1.8 ^{65}Ni peak at $1482keV$

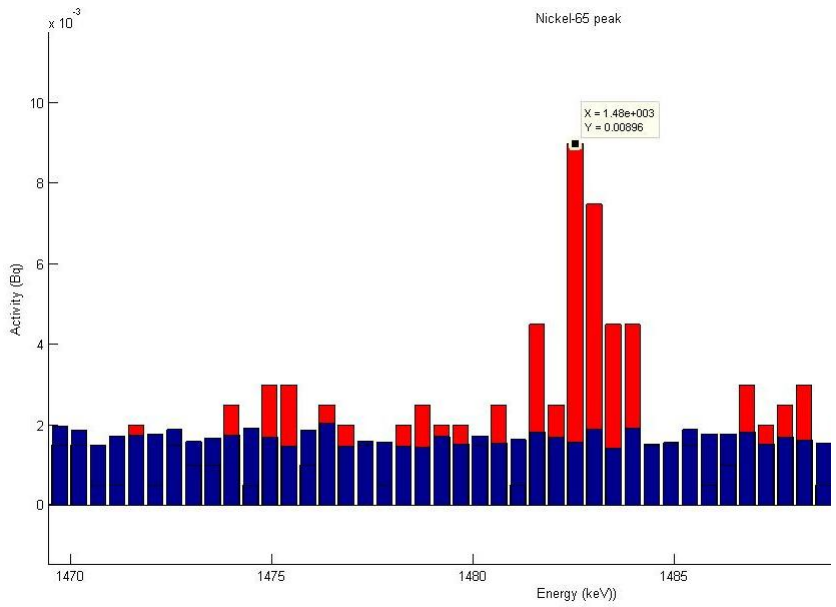

Figure 9: A graph to show the $1482keV$ peak caused by the decay of^{65}Ni.This peak appeared in the34 minute measurement.

5.1.9 ^{198}Au peak at $412keV$

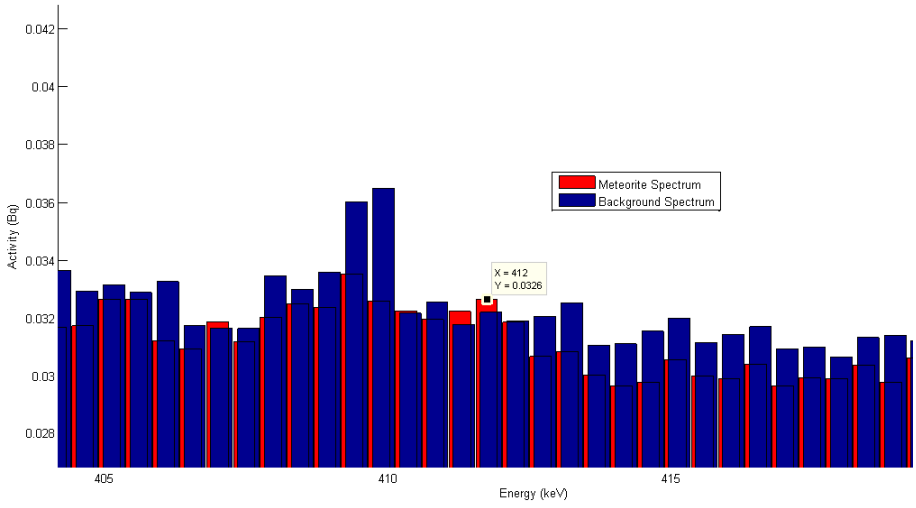

Figure 10: A graph to show the $412keV$ peak caused by the decay of^{198}Au. This peak appeared in the long 44 hour measurement.

5.2 Unusual Results

The energy peaks shown below were unusual in the way that they could not have possibly been emitted by radioactive isotopes caused by neutron capture. Instead, it seemed that radiactive isotopes from which these gamma rays were emitted had been created by the knocking out of one of the protons from the nucleus whilst absorbing the neutron (fast neutron activation). This means that the radioactive isotope is one step beneath and one to the right of the stable isotope in the nuclide chart. The cause of this could be that the meteorite was situated very close to the neutron source; perhaps the water failed to moderate a proportion of the neutrons sufficiently over such a short distance, meaning that some neutrons may had high energies compared to the moderated thermal neutrons.

5.2.1 ^{54}Mn peak at $835keV$

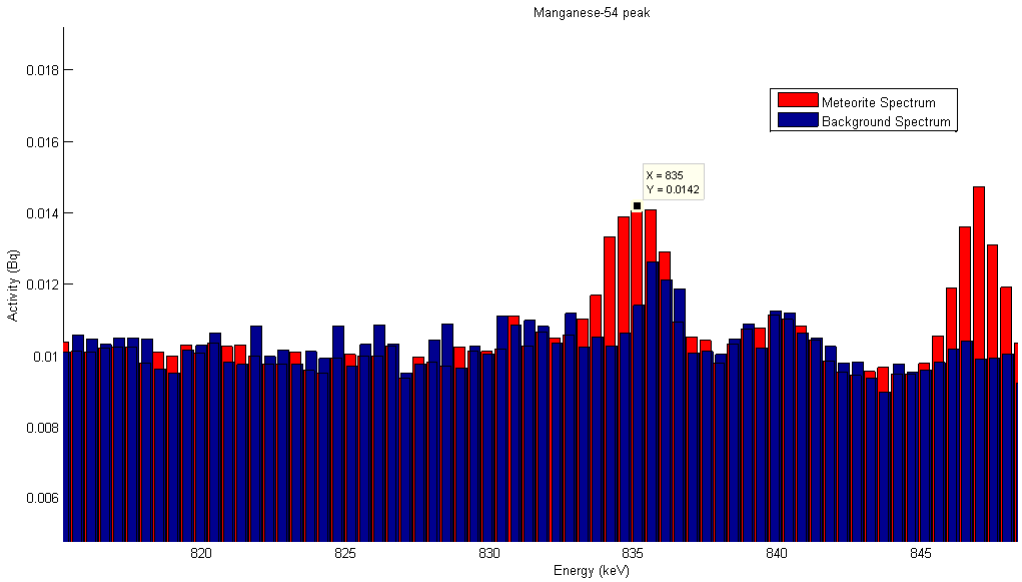

Figure 11: A graph to show the $835keV$ peak caused by the decay of^{54}Mn. This peak appeared in the long 44 hour measurement.

5.2.2 ^{58}Co peak at $811keV$

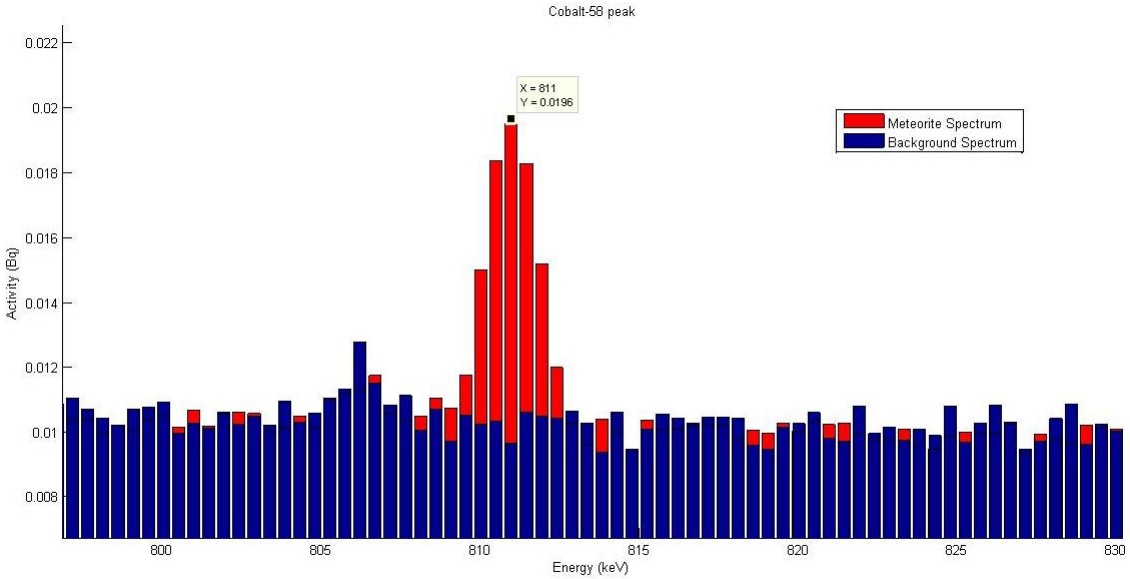

Figure 12: A graph to show the $811keV$ peak caused by the decay of ^{58}Co. This peak appeared in the long 44 hour measurement.

5.3 Summary of Results

Energy at which Peak was found (keV)	Isotope from which peak Originates	Type of Neutron Activation	Isotope of which Presence is Indicated in Meteorite
412	^{198}Au	Thermal	^{197}Au
847	^{56}Mn	Thermal	^{55}Mn
1100	^{59}Fe	Thermal	^{58}Fe
1116	^{65}Ni	Thermal	^{64}Ni
1173	^{60}Co	Thermal	^{59}Co
1292	^{59}Fe	Thermal	^{58}Fe
1333	^{60}Co	Thermal	^{59}Co
1482	^{65}Ni	Thermal	^{64}Ni
1812	^{56}Mn	Thermal	^{55}Mn
811	^{54}Mn	Fast	^{54}Fe
835	^{58}Co	Fast	^{58}Ni

Table 1: A Table to summarize the Peaks that were Found when comparing Gamma Spectra from the Meteorite with the Background Spectrum and the Radioactive Isotopes that the Peaks originate from. The table also shows the type of neutron activation that resulted in the radioactive isotope, and from which isotope the radioactive isotope 'stems' (the isotopes present in the meteorite).

5.4 Calculation of Quantities of Elements in Meteorites

With the knowledge that the meteorite weighs $88.4g$, the masses that all the different elements constitute in the meteorite can be established. The method for doing so takes into consideration many properties of the isotopes e.g. abundance, intensity of rays, half life, neutron capture cross section, duration of measurement, relative atomic mass of the corresponding elements etc. The method is explained in the appendix.

Element	Percentage Mass of Meteorite (%)	Mass (g)
Iron	98	87
Nickel	0.7	0.6
Cobalt	1	0.8
Manganese	0.004	0.003
Gold	0.00002	0.00002

Table 2: A table to show the masses of different elements in a meteorite, as determined experimentally.

6 Conclusion

The meteorite in question contained $87g$ of iron, $0.6g$ of nickel, $0.8g$ of cobalt, $0.003g$ of manganese and $0.00002g$ of gold.

7 Discussion

The conclusion reached from this experiment is only partially coherent with the hypothesis. Iron is indeed responsible for the majority of the meteorite's mass, but the mass of nickel found was much lower than expected. The quantities of cobalt and gold, however, were close to the expected values. Somewhat of an unexpected result was the presence of $0.003g$ of manganese in the meteorite.

The quality of the data achieved from this investigation could have been impaired by several factors.

Firstly, in order to calculate the masses of the different substances in the meteorite, it was assumed that the isotopic abundance in the meteorite is the same as that on Earth. This is not strictly true and is a crude assumption; the isotopic abundance present in the meteorite does not necessarily have to be the same as that on Earth. The use of an inaccurate isotopic abundance in the calculations could have distorted the final results.

Furthermore, the database values used for the calibration of the spectra and also the calculations of the masses of the elements in the meteorite had uncertainties that were not accounted for in this text. This uncertainty in the data could have contributed to the deviation from the general consensus that coarse iron octahedrites contain 6.5% to 8.8% nickel.

Another potential weakness in the investigation was perhaps the fact that measurements on the meteorite were only conducted for a duration of 44 hours. This could have influenced the detection of the potential presence of isotopes with particularly long half lives; the peaks for these isotopes will not have had sufficient time to appear with statistical significance.

Moreover, when observing the graphs it is clear that the activity of the background radiation present in the meteorite spectrum is systematically lower than that of the activity in the 'background spectrum'. This is due to the shielding effect that the meteorite causes when it is placed in front of the detector; it blocks some of the background radiation from reaching the detector. The peaks in gamma radiaition visible in gamma spectroscopy graphs are unique to each isotope, but nevertheless there are radioactive isotopes with very similar energies of gamma emissions. These similar energies could be grouped as the same energy depending on the resolution of the germanium detector and the software used to process the spectra. This could pose a problem in the detection of peaks when analysing the spectra with the technique used in this investigation. Figure 10, for example, makes it seem as if background radiation as well as radiation from the ^{198}Au isotope in the meteorite is emitted at an energy of $412keV$. In reality, however, there is next to no background radiation at the exact energy at which ^{198}Au emits gamma radiation ($411.80205keV \pm 0.00017keV$[8]), but the graphing software 'groups' this energy with other similar energies so that they are represented by the same peak. For this reason, a reduction in the

background radiation detected by the detector when performing measurements on the meteorite could imply reductions in peaks that also represent gamma rays emitted by the meteorite. This is an issue because the peaks become more difficult to detect and analyse and it is possible to mistake significant peaks for background radiation. What's more, the area under the peaks is used in the calculations of the quantities of the elements and naturally, the peak size affects the area of the peak meaning that the results for how much of the meteorite each element represents could be affected and unreliable. A slight improvement could be made by graphing the spectra as continuous graphs instead, giving much more precise measurements of the energies at which radiation is emitted and thus improving the chances of being able to discern background radiation from the radiation that the meteorite emits.

8 Acknowledgements

I would like to thank my colleague, Henrik Norström, for his cooperation in the experiments and the analysis of the data. I would also like to thank my mentor, Professor Bo Cederwall of the Department of Nuclear Physics at the Royal Institute of Technology, who provided great help and guidance throughout the research project and whose assistance was imperative to the development of the project. Many thanks also go to Henrik Skogby from the Natural History Museum in Stockholm for the kind provision of the meteorite used in the investigations.

References

[1] MIT. Meteorites. http://web.mit.edu/course/12/12.004/TheLastHandout/PastHandouts/Chap02.Meteorite Last modified: 21 February 2001

[2] Lodders, K., Palme H., & Gail, H.P. Abundances of the Elements in the Solar System. http://arxiv.org/ftp/arxiv/papers/0901/0901.1149.pdf Date published: 2009

[3] Bottke, W.F., & Martel, L.M.V. Iron Meteorites as the Not-So-Distant Cousins of Earth. http://www.psrd.hawaii.edu/July06/asteroidGatecrashers.html Date published: 21 July 2006

[4] McDonough, W.F. (R. Teisseyre and E. Majewski, Eds.) The Composition of the Earth. http://quake.mit.edu/hilstgroup/CoreMantle/EarthCompo.pdf Date published: 2000.

[5] Paul, D.A.L (Bailey, D. Ed.) The Germanium Spectrometer. http://www.physics.utoronto.ca/~phy326/ge/Germanium.htm Date published: September 1994. Last modified: June 1998.

[6] Budka, P.Z., Viertl, J.R.M., Thamboo, S.V., & Schiffman, R.A. Gravity Independent Macro/Micro-Structural Features http://meteormetals.com/pub/EMMS_1995.PDF Date published: 1995

[7] Korotev, R.L. Meteorite or Meteorwrong? http://meteorites.wustl.edu/id/metal.htm Last modified: 24 August 2010

[8] Chu, S.Y.F., Ekström, & L.P., Firestone, R.B. The Lund/LBNL Nuclear Data Search. http://nucleardata.nuclear.lu.se/nucleardata/toi/radSearch.asp Last modified: February 2009.

[9] National Nuclear Data Centre, Brookhaven. Chart of Nuclides. http://www.nndc.bnl.gov/chart/

[10] Canadian Coalition for Nuclear Responsibility. Here are the Radioactive Byproducts of Depleted Uranium (Uranium-238). http://www.ccnr.org/decay_U238.html

[11] Canberra Industries. Germanium Detectors - User's Manual. http://www.aps.anl.gov/Xray_Science_Division/Optics_and_Detectors/Detector_Pool/Detector_Information/Ca Last Modified: 1 April 2003

[12] Storr,W. The Junction Diode. http://www.electronics-tutorials.ws/diode/diode_3.html. Last modified: July 2011.

Appendix

A The Construction of the Efficiency Curve (Figure 1)

To be able to construct an efficiency curve, the multi-channel analyzer program used to obtain the spectra - Maestro-32 - first had to be calibrated.

Calibration of Maestro-32

To calibrate Maestro-32 with the germanium detector, a sample of ^{137}Cs was used. ^{137}Cs is an ideal candidate for initial calibration because it creates two distinct peaks at $32.194keV$ and $661.657keV$, where the peak at $32.194keV$ is an X-ray emission[9]. These two peaks, therefore, were used to initially calibrate the channel number with the energy of the photons/gamma rays. To further improve the accuracy of the calibration, decay charts of naturally occuring decay chains (such as the one shown here originating from^{128}U [10]) were used to search Lund's Nuclear Database to identify peaks in the background spectrum, allowing for the calibration of more peaks with accurate values and thereby achieving a more reliable calibration.

Construction of the Efficiency Curve

Samples of ^{60}Co, ^{133}Ba and ^{137}Cs of which the activities at a certain point in time were known, were placed next to the germanium detector and a gamma spectrum of their emissions was produced through measurement with Maestro-32. Because their activities had been established at a previous time (A_0), their actual activities (A) at the time of measurement (t is the time in seconds after the determination of the first 'known activity') could be determined using the following formulae:

$$A = A_0 e^{-\lambda t} \tag{1}$$

$$\lambda = \frac{ln2}{T_{\frac{1}{2}}} \tag{2}$$

Table 2 shows the activities of the samples as measured 1 October 1988 at 1200 GMT (a known point in time) and as calculated at the time of measurement:

Isotope	Activity on 1 October 1988, 1200 GMT ($10^5 Bq$)	Calculated Activity at time of measurement ($10^4 Bq$)
^{60}Co	4.01450	1.9979
^{133}Ba	3.87010	8.6015
^{137}Cs	3.90720	23.087

Table 3: A table to show the activities of the three samples^{60}Co,^{133}Ba and^{137}Cs, at a known point in time and as calculated using (1) and (2) at the time of measurement (8334 days after).

The values in the second column of Table 2 are the 'actual' activities of the isotopes.

Because each isotope emits gamma radiation at one or more different energies, the 'intensity' of that energy must be taken into consideration. Consider, for example, the imaginary isotope $^{\mathrm{m}}Aa$ which has an activity, D. $^{\mathrm{m}}Aa$ emits gamma rays at $'x'keV$ and $'y'keV$. 60% of all the gamma rays are $'x'keV$ and 40% are $'y'keV$. This means that the 'activity' at $'x'keV$ is $0.6 \times D$ and the 'activity' at $'y'keV$ is $0.4 \times D$. Therefore, the actual activity of each gamma ray (graphically visible as a peak in a spectrum) was its intensity multiplied by the activity of the isotope.

To obtain the activity of the individual peaks from each isotope, the net area under the peaks was taken (Maestro-32 has a function for this) and divided by the time taken for the measurement. These values gave the activities of the isotopes and gamma rays as determined by the detector.

The activities as measured by the detector were divided by the corresponding 'actual' activities to give the ratio between the two values. These values were then plotted on the y-axis against the matching energies (gamma rays) to give the graph seen in Figure.1.

B Germanium Detectors

Germanium detectors are high resolution semi-conductor diodes in which there are three three regions: P-I-N. The 'I' or 'intrinsic' region is that which is sensitive to ionizing radiation such as X-rays and gamma rays. The intrinsic region is found between the P and N electrodes and is sometimes also called the depleted region[10]. Upon application of a negative voltage (reverse bias), the distance between the P and N electrodes increases and an electric field runs over the depleted region [10, 11]. Photon interaction in the intrinsic region causes charge carriers to be produced and these charge carriers travel along the electric field to the corresponding P and N electrodes. The charge of these carriers is proportional to the energy carried by the photons and can therefore be transformed into an electrical pulse by a "charge-sensitive preamplifier" that can be later manipulated to produce a gamma spectrum.

C Experimental Set Up

Neutron Source

The neutron source consisted of a pellet containting Californium-252 (^{252}Cf) which is a spontaneous fission source that emits neutrons. It was submerged in a water tank to moderate the neutrons and thereby increase the probability that they would be absorbed by the nuclei in the meteorite.

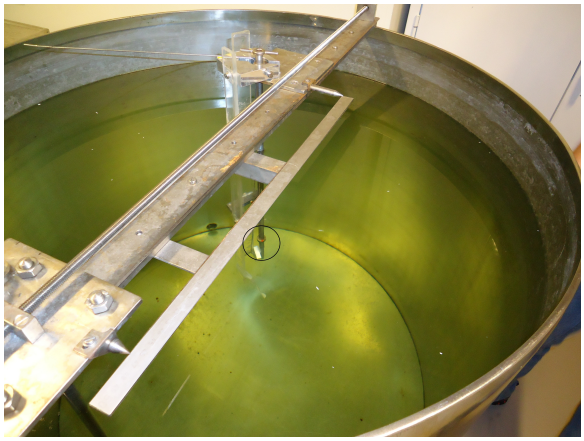

Figure 13: A photograph to show the^{252}Cf neutron source (ringed in black) submerged in a water tank

The meteorite was placed near the neutron source with the help of a metal 'cage' and a plastic device which was submerged into the water.

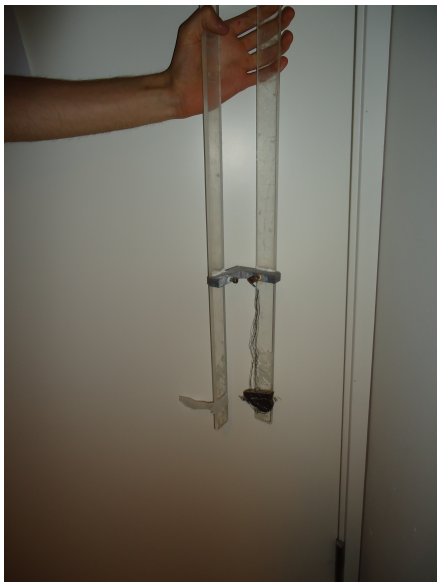

Figure 14: A photograph to show how the meteorite was attached to the plastic device with the help of a stainless steel wire cage.

Germanium Detector

Figure 15: A Photograph to show the Germanium Detector used in the Investigation

D Calculation of Mass of Elements in Meteorite

If formula (1) in Section A is integrated it represents the area beneath a curve on an Activity-Time graph between two points :

$$Area = A_0 \frac{e^{-\lambda t_1} - e^{-\lambda t_2}}{\lambda} \tag{3}$$

A simple rearrangement of this equation gives:

$$A_0 = \frac{Area \cdot \lambda}{e^{-\lambda t_1} - e^{-\lambda t_2}} \tag{4}$$

The area of a single peak in a gamma spectrum is comparable to the area beneath a curve on an Activity-Time graph between two time points. The area of a single peak of an isotope can therefore be used to calculate the activity at the start of measurement (if the half-life of the isotope is known). With the knowledge that the activity of a substance is the product of λ and the number of nuclei it contains,

$$A_0 = \lambda \cdot N \tag{5}$$

, dividing $A_0$by λ will give the number of nuclei at the start of measurement. Immediately doing this, however, will not give the number of nuclei of a certain element in the meteorite at the start of measurement. Instead, the value of 'N' represents the number of nuclei emitting gamma radiation at the same energy as the peak. The results clearly have to be 'standardized'. It is here that the efficiency curve detailed in Section A comes into the picture. The energy of the peak is located along the x-axis and then the corresponding 'factor of efficiency' is found on the y-axis. The value of 'N' is divided by this factor of efficiency.

Further 'standardization' is still required. This is done by dividing the new value of N by the percentage intensity that the specific/peak gamma ray represents in the whole isotope to represent all the gamma rays from that isotope. This value represents the number of nuclei of that particular isotope that were present in the sample, N_I. Different isotopes, however, have different probabilities of absorbing neutrons called the 'absorption cross section' and to account for this, N_I is divided by the absorption cross section value. To achieve a value that represents the number of nuclei of the corresponding element, the previous value must be divided by the percentage abundance of that isotope for the whole element. Call this new value 'N_E '.

It is crucial to keep in mind that the number of nuclei of an element is not the only factor affecting the percentage mass of the meteorite that the said element is responsible for. The element's relative atomic mass (A_r)must also be taken into consideration by dividing N_E by the element's A_r. For simplicity, call this value the comparison mass: C_m . If the C_m of all the elements present in the meteorite are found, they can be compared.

This comparison is made by dividing one element's $C_m$value by the sum of all the elements' $C_m$values and multiplying by 100. A percentage value is now given for the mass of the element in the total mass of the meteorite. This is repeated for all the elements.

When the percentage quantities are found, all that remains is to multiply them by the mass of the meteorite to obtain the mass of the element present in the meteorite.

Activated Isotope (present in meteorite)	Fe-58	Mn-55	Co-59	Ni-64	Au-197
Radioactive Isotope	Fe-59	Mn-56	Co-60	Ni-65	Au-198
Energy of Gamma Ray (keV)	1099	847	1173	1482	412
Abundance	0,3%	100,0%	100,0%	0,9%	100,0%
Half life d	44,50		1925,28		2,70
Half life h		2,58		2,52	
Half life s	3844368,00	9284,04	166344192,000	9061,92	9720,00
Net area	551,00	731,00	2513,00	40,00	720,00
Normalized net area	558,75	741,77	2548,35	40,59	730,13
Intensity	0,57	0,99	1,00	0,24	0,96
Absorption cross section	1,15	13,41	37,17	1,52	97,70
Live time	157011,10	2010,04	157011,10	2010,04	157011,10
Real time	159219,90	2039,66	159219,90	2039,66	159219,90
Time until measurement starts	2460,00	420,00	2460,00	420,00	2460,00
time until measurement ends	161679,90	2459,66	161679,90	2459,66	161679,90
Detected Activity (Bq)	0,004	0,50	0,02	0,02	0,06
Activity of Isotope (Bq)	0,01	0,51	0,02	0,09	0,06
Activity divided by lambda	35501,79	6794,76	3903620,93	1209,01	910,00
Above cell divided by cross section and efficiency	12359197,36	168897,73	42008296,27	318578,68	3725,71
Above cell divided by abundance	4413999057,38	168897,73	42008296,27	34403745,38	3725,71
Normalization 3	79027447,58	3074,781225	712850,7766	586094,4698	18,91222469
% of mass	98%	0,004%	1%	0,7%	0,00002%
Mass of each element (g)	87,0	0,003	0,8	0,6	0,00002

Table 4: A Table to show the Calculations of the Masses of Elements in a Meteorite